Biosensors and Bioelectronics 142 (2019) 111515

Contents lists available at ScienceDirect

Biosensors and Bioelectronics

journal homepage: www.elsevier.com/locate/bios

Separation detection of hemoglobin and glycated hemoglobin fractions in blood using the electrochemical microfluidic channel with a conductive polymer composite sensor

M.D. Mozammal Hossain[a], Jong-Min Moon[a], N.G. Gurudatt[a,c], Deog-Su Park[b], Cheol Soo Choi[c,**], Yoon-Bo Shim[a,b,*]

[a] Department of Chemistry and Institute of BioPhysio Sensor Technology (IBST), Pusan National University, Busan, 46241, Republic of Korea
[b] Institute of BioPhysio Sensor Technology (IBST), Pusan National University, Busan, 46241, Republic of Korea
[c] Korea Mouse Metabolic Phenotyping Center, Lee Gil Ya Cancer and Diabetes Institute, and Internal Medicine, Gil Medical Center, Gachon University, Incheon, 21565, Republic of Korea

ARTICLE INFO

Keywords:
Clinical diagnosis
Hemoglobin
Glycated hemoglobin
Amperometric sensor
Electrochemical microfluidic channel
Blood

ABSTRACT

Separation and detection of hemoglobin (Hb) and glycated hemoglobin fractions (HbA1c, $HbAld_{1+2}$, HbAle, HbAld3a, $HbAl_{a+b}$, HbA2, and HbAld3b) was performed using an electrochemical AC field modulated separation channel (EMSC) coupled with a sensor probe. The sensor was fabricated based on immobilization of a redox mediator on the poly(2,2′:5′,5″-terthiophene-3′-*p*-benzoic acid, pTTBA) and N,S-doped porous carbon (NSPC) nanocomposite. The different types of catalytic redox mediators such as Nile Blue (NB), toluidine blue O (TBO), and Neutral Red (NR) were evaluated to achieve the efficient detection. Of these, the NB-based sensor showed the best analytical signal for Hb and HbA1c, thus it was characterized using various electrochemical and surface analysis methods. After that, the sensor was coupled with the EMSC to achieve the separation detection of the Hb family. The frequency and amplitude of the AC electrical field applied onto the EMSC walls were the main driving forces for the separation and sensitive detection of the analytes. Under optimized conditions, linear dynamic ranges for Hb and HbA1c among their fractions were obtained between 1.0×10^{-6} to 3.5 mM and 3.0×10^{-6} to 0.6 mM with the detection limit of $8.1 \times 10^{-7} \pm 3.0 \times 10^{-8}$ and $9.2 \times 10^{-7} \pm 5 \times 10^{-8}$ mM, respectively. Interference effects of other biomolecules were also investigated and the clinical applicability of the device was evaluated by the determination of total Hb and % HbA1c in real human blood samples.

1. Introduction

Hemoglobin (Hb) has an important physiological role in human blood as a carrier of oxygen molecules (O_2) (Weissbluth, 1974; Hussain et al., 2017). This tetrameric protein consists four polypeptide subunits (two α - and two β - globins), and each one bounds non-covalently to the prosthetic oxygen-binding heme group. Hb is glycated in certain level; approximately 95% of the major form of Hb is HbA (α2β2), others are HbA_2 (α2δ2, < 3.2%) and fetal Hb (HbF, α2γ2, < 1%) in normal adults. Minor variants of Hb have also been identified as hemoglobin A1a (1.6%), A1b (0.8%), and A1c (3–6%), A1d, and A1e according to their carbohydrate moiety which are also present in normal human blood (Abraham, 1981). Low levels of Hb have been found in anemic patients and it is also related to various clinical complexities (Jing et al., 2012). Otherwise, glycated hemoglobin (HbA1c) is clinically important as its concentration is directly or indirectly linked with various diseases including diabetes, nephropathy, retinopathy, atherosclerosis, and other perivascular diseases. Recently, it has been found that the higher HbA1c level is associated with clinical outcomes in diabetic patients and chronic kidney diseases (Kuo et al., 2016).

Various methods are available to determine Hb or HbA1c, including ion-exchange chromatography (Lafferty et al., 2002), capillary electrophoresis (Dong et al., 2013), immunoassays (Ang et al., 2016), and spectroscopy (Barman et al., 2012; Kiran et al., 2010). These methods are valuable, however they are time consuming, require large sample solution, and need trained person, hence they cannot be applied for the point-of-care application due to its inability of miniaturization. Generally, both the HbA1c and Hb concentration in the same blood sample

* Corresponding author. Department of Chemistry and Institute of BioPhysio Sensor Technology (IBST), Pusan National University, Busan, 46241, Republic of Korea.
** Corresponding author.
E-mail addresses: cschoi@gachon.ac.kr (C.S. Choi), ybshim@pusan.ac.kr (Y.-B. Shim).

https://doi.org/10.1016/j.bios.2019.111515
Received 1 July 2019; Accepted 13 July 2019
Available online 15 July 2019
0956-5663/

should be analyzed to determine the HbA1c content. In addition, Hb and Hb fractions may interfere to the HbA1c analysis, which can potentially result in unsuitable clinical management (Rhea and Molinaro, 2014). Therefore, simultaneous detection of HbA1c and Hb among their derivatives using a minimal quantity of blood sample is of great importance. To date, few electrochemical sensors have been developed for the detection of both HbA1c and Hb based on impedance measurement with a mediated ring-shaped interdigital electrode (Hu et al., 2014) or using a dual-sensor formatted-aptamer sensor (Moon et al., 2017). In this case, two or more sensors are combined them together to detect HbA1c and Hb, which require multistep processing, careful handling, and importantly they are not entirely robust. Thus, it is essential to develop a portable sensor device for simple detection of them, simultaneously.

A microfluidic device integrated with an electrochemical sensor is beneficial due to its unique ability in the clinical separation analysis in terms of low cost, high selectivity, low sample volume, and ability to detect target molecules (Lee et al., 2008; Kumar, 2010). They are also considered to be the next generation bioanalytical systems for global human health monitoring in personalized settings (Sackmann et al., 2014; Dincer et al., 2017; Demirci et al., 2017). Among various types of microfluidic devices, recently electrochemical AC field modulated separation channel (EMSC) has received much attention due to its robustness, extremely high separation efficiency, facile fabrication, and low cost (Noh et al., 2012; Hussain et al., 2018). Furthermore, the integration of an amperometric sensor on the channel exit is preferred due to its high sensitivity and selectivity, which greatly reduces the interferences of biomolecules present in the real sample matrix (Hussain et al., 2018). Therefore, we have tried to develop a potential modulated separation channel integrated with an amperometric sensor for the detection of glycated Hb fractions and Hb in a single experimental setting, and the redox ability of heme group mediated by Nile blue (NB) immobilized on the sensor probe. To enhance the sensitivity and stability of device, a redox mediator NB was covalently attached to the polymeric chain of pTTBA and interspersed with N, S-doped porous carbon ((NSPC) to form composite films. Porous materials have been widely applied, in particular as electrode materials due to facilitation of electron transfer kinetics (Borchardt et al., 2017). Of them, heteroatom doped porous carbons have been recently prepared as electrode catalytic materials, where incorporated heteroatoms can cause the extra-electron distribution which lead to the enhancement of catalytic properties (Naveen et al., 2017; Zhu et al., 2016). Thus, we have introduced NSPC into the conducting polymer composite to achieve the improvement of sensitivity and stability of the sensor probe.

In the present study, we report a highly sensitive and selective method that enables the separation of Hb and glycated Hb fractions ($HbAld_{1+2}$, HbAle, HbAld3a, $HbAl_{a+b}$, HbA2, and HbAld3b) using the EMSC, followed by their detection with NB anchored-conducting polymer composite with NSPC. The sensor surface was characterized using cyclic voltammetry (CV), X-ray photoelectron spectroscopy (XPS), quartz crystal microbalance (QCM), field-emission scanning electron microscopy (FE-SEM), and electrochemical impedance spectroscopy (EIS). Separation parameters (AC field parameters *i.e.* frequency and amplitude) and analytical parameters (NB concentration, pH, temperature, reaction time) were optimized and the detection limits of HbA1c and Hb were evaluated. Individual HbA1c and Hb contents among their fraction in blood samples were determined to demonstrate the real clinical values. The selectivity of the sensor was also examined toward various biomolecules present in the real sample matrix.

2. Experimental

2.1. Materials and instruments

NSPC was synthesized according to the Zn MOF preparation procedure (Naveen et al., 2017) as follows; two solutions were separately prepared by dissolving 0.456 g of Zn acetate (Sigma) with 0.5 g polyvinyl pyrrolidone (PVP) and 0.250 g of dithiooximide (DTO, Sigma) in 50 mL of dimethyl formamide (DMF) and mixed under stirring at 80 °C for 1 h. The yellow precipitate, ZnDTO was collected by centrifugation (8000 rpm, 10 min) and washed with an aqueous solution of 37% HCl several times to remove unstable and inactive Zn nanoparticles. Remaining HCl was completely washed with distilled water and ethanol, and kept in vacuum dry oven (50 °C) overnight. For the carbonization, dried particles were placed in a tube furnace and heated at 900 °C for 3 h under nitrogen gas flowing to obtain NSPC.

The standard HbA1c solution (JCCRM 411) was purchased from the Reference Material Institute for Clinical Chemistry Standards (Kawasaki, Japan). For the separation experiment, the inside of the channel device was cleaned alternately with 0.1 M HCl and distilled water for 30 min, followed by equilibrating the separation channel with the running buffer prior to the injection of Hb and HbA1c samples. Human blood samples were collected from healthy volunteer subjects into heparinized collection tubes as anticoagulant and immediately stored at 4 °C until a hemolysate was prepared. Other required materials and instruments for the experiments can be found in Supplementary information Section 1.1.

2.2. Fabrication of sensor probe and microfluidic device

The EMSC was fabricated following our previously reported method with slight modification (Noh et al., 2012), which was prepared using carbon ink on the glass slides by a screen printer. A positive type photomask with the channel structure was designed using a computer-aided design software package (Autocad; AutoDesk, San Rafael, CA, USA), transferred onto a patterned stencil (designed by Sejin Tech, South Korea). The fabricated channel length was 52.0 ± 0.5 mm and the width was 95.0 ± 2.5 μm.

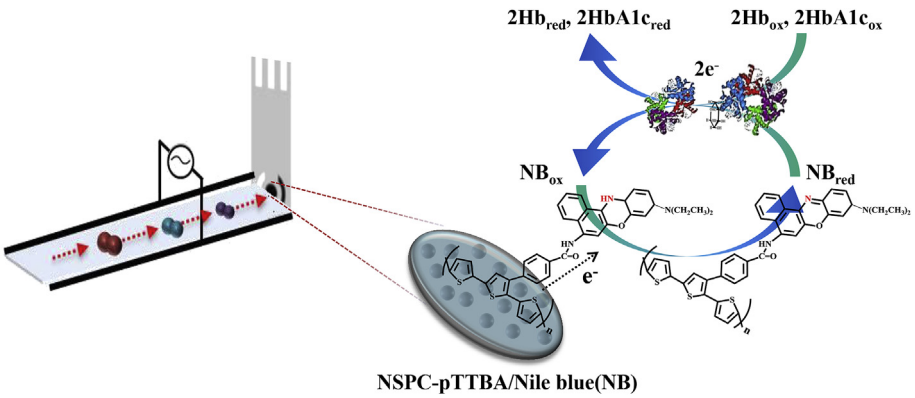

Scheme 1. Schematic diagram represents the fabrication of the Hb and HbA1c sensor and the detection method.

The fabrication process of the sensor probe is presented in Scheme 1. Firstly, the NSPC solution (0.5 mg/mL) was prepared in acetonitrile and sonicated (350 W, 40 kHz) for 1 h to obtain a homogeneous dispersed solution. Next, the 0.1 mM TTBA monomer was added in the same solution and sonicated (350 W, 40 kHz) for 2 h. Thereafter, 0.3 μL of the TTBA-NSPC suspension was drop casted onto the SPCE and dried for 15.0 min at 40 °C. Next, the nanocomposite film was formed onto the SPCE surface by cycling the potential between 0.0 to 1.0 V in 0.1 M PBS (pH 7.4) at a scan rate of 50 mV/s. During the potential cycling, the adjacent monomer molecules form weak bonds (overlapping of π-orbitals) with each other to form a polymer layer. Since, the NSPC is present intermittently, it forms a nanocomposite film with the polymer layer. After polymerization, the NSPC-pTTBA modified electrode was immersed in 10.0 mM EDC/NHS solution prepared in 0.1 M PBS (pH 7.4) for 6 h to activate the benzoic acid groups of the nanocomposite surface. Then, the NSPC-pTTBA probe was incubated with 1.5 mM NB solution prepared in 0.1 M PBS (pH 7.4) for 12 h at room temperature to form the final sensing probe as NSPC-pTTBA/NB.

3. Results and discussion

3.1. Electrochemical characterization of mediators and sensor probes

Prior to fabrication of final sensor probe, the sensor response according to the different kinds of electron transfer mediators (NB, toluidine blue O (TBO), and neutral red (NR)) was evaluated based on redox behaviors of them. As shown in Fig. 1(A-C), CVs recorded for TBO, NR, and NB immobilized sensor layers exhibited enhanced well-defined redox peaks of Hb at the potentials (TBO: −320/-290 mV, NR: −640/-600 mV, and NB: −420/-380 mV), respectively. They reveal that the performance of each electrode is different according to the kind of mediators. The enhanced reduction currents mediated by TBO, NR, and NB are observed as 1.86, 2.12, and 3.48 μA for Hb and 1.22, 1.34, and 2.78 μA for HbA1c, respectively. The results indicate that the NSPC-pTTBA/NB probe has the highest catalytic response to Hb and HbA1c when compared with TBO and NR immobilized ones, and it has been used for subsequent experiments.

Fig. S1(A) shows the CVs recorded for the NSPC-pTTBA/NB sensor at the scan rate between 25 and 175 mV/s in 0.1 M PBS. Both I_{pc} and I_{pa} were directly proportional to the scan rate, indicating the redox process was controlled by surface confined NB. According to the following equations: $Q = nFA\Gamma$, the surface coverage ($\Gamma = 5.58 \times 10^{-11}$ mol/cm^2) of NB could be obtained by integrating the area under the cathodic peak, and the electron transfer number ($n = 1.92$), implying that the NB was formed in surface layer. Depending on the number of protons involved in the redox reaction, the formal potential changed according to the electrolyte pH. With increasing pH in the range of 4.0–9.0, both E_{pa} and E_{pc} of NB shifted to the negative direction (Fig. S2), and corresponding ΔE/ΔpH was −61 mV/pH. The result suggests that the redox reaction of mediator possessed the two-electron and two-proton process.

EIS experiments were carried out to investigate the electrical property of sensor as shown in Fig. S1(B), which shows the representative Nyquist plots obtained at the open-circuit voltage for each layer of the sensor in 0.1 M PBS. The charge-transfer resistance (R_{ct}) values were determined by fitting the experimental data with the Randle circuit (inset of Fig. S1(B)) employing the Zview2 impedance software. The bare SPCE shows the R_{ct} value of 33.4 ± 2.9 kΩ (blue curve), and it drastically decreases to 7.6 ± 0.6 kΩ (black curve) (> 4 times) when the NSPC-pTTBA composite layer is formed on the bare SPCE. The decrease in the R_{ct} value clearly indicates the enhanced electron transfer property of the modified surface. After immobilization of NB, the R_{ct} slightly increased to 11.2 ± 1.6 kΩ (red curve), due to the covering of the less conductive NB on the sensor surface. The NB is crucial to obtain the enhanced analytical signals for Hb and HbA1c detection. Hence, we also investigated the QCM to confirm binding quantity of NB on the NSPC-pTTBA surface during immobilization. The overall frequency change was (Δf) of 35 ± 2 Hz after 33.0 min with a calculated mass change of (Δm) of 38.47 ± 6.32 ng. Detailed experimental information is given in the supporting information.

3.2. Surface characterization of the sensor probe

To investigate the surface characterization of the NSPC, NSPC-pTTBA, and NSPC-pTTBA/NB layers, FE-SEM experiments were performed. The images show that the uniform spherical shape of NSPC as-

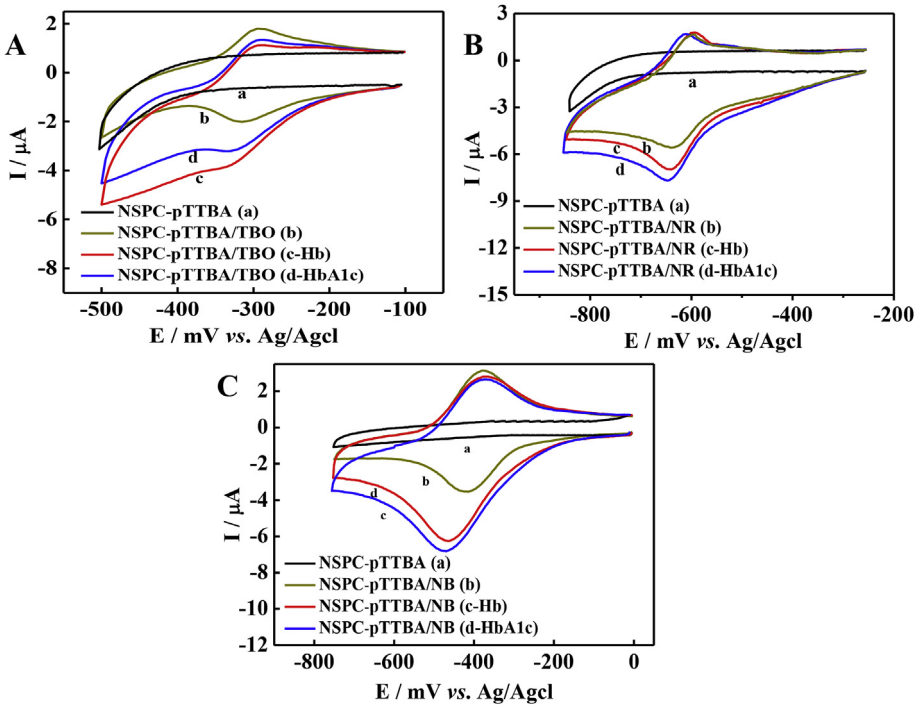

Fig. 1. CVs recorded using (A) NSPC-pTTBA/TBO, (B) NSPC-pTTBA/NR, and (C) NSPC-pTTBA/NB modified electrodes in 0.1 M PBS containing Hb and HbA1c.

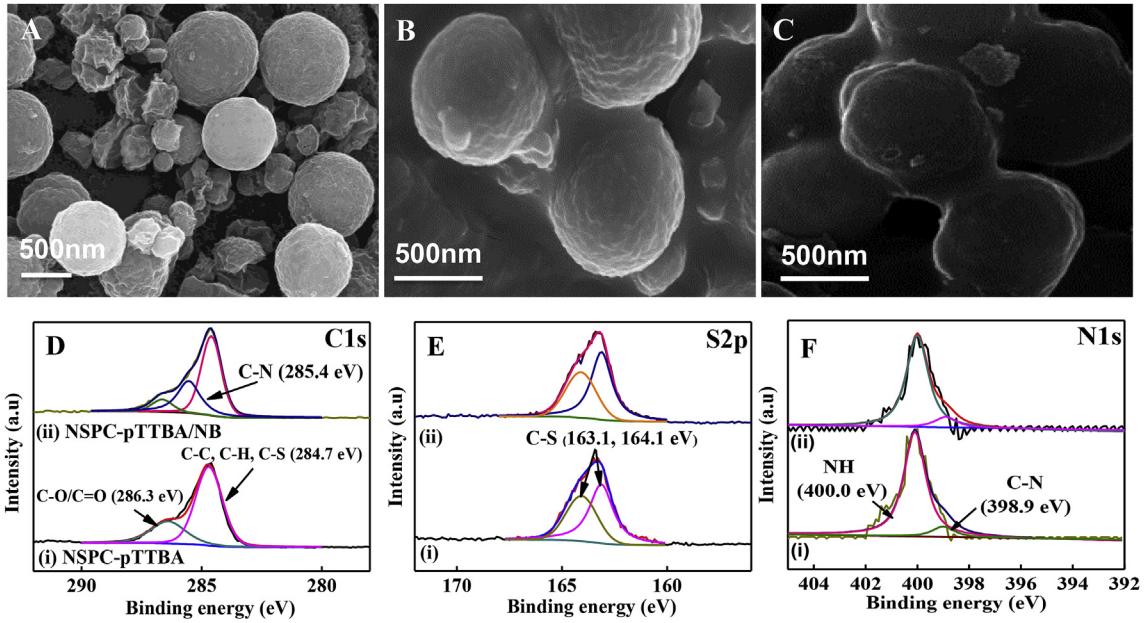

Fig. 2. FE-SEM images of (A) NSPC, (B) NSPC-pTTBA composite layer, and (C) NSPC-pTTBA/NB. (D) XPS spectra of the (B) C1s, (C) S2p, and (D) N1s for (i) NSPC-pTTBA and (ii) NSPC-pTTBA/NB layers.

prepared in the size of around 900 ± 100 nm, (Fig. 2(A)), while the NSPC-pTTBA displayed a polymer network covering on the sensor surface (Fig. 2(B)). When NB was chemically attached on the pTTBA, a dense covering was observed (Fig. 2(C)). To illustrate chemical bonding of the modifiers immobilized on each layer of the sensing probe, XPS spectra were obtained for the layers after 50 s etching with Ar gas ion, and they were standardized with a C1s peak at 284.7 eV as an internal standard. Fig. 2(D-F) displays the deconvoluted spectra for (i) NSPC-pTTBA and (ii) NSPC-pTTBA/NB layers. The C1s spectrum for NSPC-pTTBA layer reveals the peaks at 284.7 eV (C–C, C–H, and C–S bonds) and 286.3 eV (C–O and C═O bonds), owe to the presence of carbon and sulfur atoms in pTTBA (Fig. 2(D)). After immobilizing NB on the NSPC-pTTBA layer, an additional peak is observed at 285.4 eV owing to C–N bond formation between pTTBA and NB. This peak, however, is not appeared for the mere NSPC-pTTBA layer, indicating that the peak was appeared by the successful immobilization of NB. The S2p spectra of both layers showed clear two peaks at 163.1 and 164.1 eV due to the presence C–S bond of the NSPC and pTTBA (Fig. 2(E)). The deconvoluted N1s spectra for NSPC-pTTBA/NB surface show peaks at 398.9 and 400.1 eV because of the covalent bond formation between –COOH groups of pTTBA and –NH_2 groups of NB (Fig. 2(F)). The results clearly indicate the successful formation of NSPC-pTTBA composite layer and covalent immobilization of NB.

3.3. Separation detection of Hb and glycated Hb using EMSC

After optimizing the analytical condition, we integrated the NSPC-pTTBA/NB sensor probe on the exit of the fluidic channel precisely as shown in Scheme 1. The detection of MetHb, Hb, and HbA1c at −500 mV *vs.* Ag/AgCl was representatively examined using a standard sample. In the first step, we monitored signal in two conditions (i) without and (ii) with AC potential application as shown in Fig. 3(A). Without AC potential application, response peak was observed but it was not separated (Fig. 3(A)(i)), while three response peaks were observed in the electropherogram (Fig. 3(A)(ii)) at migration times of 191.1 ± 0.5, 211.4 ± 1.0, and 231.7 ± 1.5 s ($n = 5$) when the AC potential was applied, indicating the separation of MetHb, Hb, and HbA1c. The AC field application on the channel walls produced an oscillation and fluctuation of the analytes in the channel, which resulted in the separation of samples according to the molecular weight (Noh et al., 2012). Small molecules fluctuate fast and move towards centered position, while large molecules fluctuate slowly, resulting in the enhancement of separation efficiency. We also performed the optimization experiment to determine the separation parameters, in terms of AC frequency, amplitude, flow rate, and the effect of ionic strength to achieve the best separation condition. The effect of the AC frequency was investigated between 1.0 and 10.0 MHz at the constant flow rate (Fig. 3(B)). As shown in the electropherogram, the peaks were separated between 1.0 and 4.0 MHz, however, the migration time for the peaks was very close, which is not favorable for their selective detection in the samples. Therefore, we examined high frequency at 6.0, 8.0, and 10.0 MHz, where three distinct peaks with distant migration time were observed in all experimental conditions; however, the separation time was shortest at 6.0 MHz. Hence, we used 6.0 MHz AC frequency in further experiments. The amplitude of the AC field is another parameter that affects the separation process. Thus, the amplitude of AC potential was studied to 1.0, 2.0, and 3.0 V, as shown in Fig. 3(C). The best efficiency was observed at 2.0 V and this potential was used in the subsequent experiments. To separate the target species effectively, we also optimized the flow rate from 3.0 to 10.0 μL/min (Fig. 3(D)). At higher flow rate between 10.0 and 8.0 μL/min, the separation of the target molecules were not clearly discrete, however, they were completely separated at the flow rates between 7.0 and 3.0 μL/min. The target species were separated in the shortest time at 6.0 μL/min, which was used in the subsequent experiments.

We studied for the concentration and pH dependency of electrolyte for the sample separation, because they could act as an important role of dynamic interaction of the analytes on the channel wall (Tseng et al., 2000). Fig. S4(A) shows the effect of the buffer concentration (50, 100, 200, and 400 mM) on the separation of Hb and HbA1c. The separation was accomplished within 4 min, and there was no difference in peak value from 100 to 400 mM (Fig. S4(A) inset), but remarkably longer time was needed using 50.0 mM buffer. To elucidate the effect of pH on Hb and HbA1c separation, the electrophoregram was obtained at different pH values (5.5, 7.4, and 8.5) using 100 mM buffer. The shortest separation time and high sensitivity were observed at pH 7.4 (Fig. S4(B)).

To confirm the migration time of Hb, MetHb, and HbA1c, we performed two control experiments. At first, only Hb was injected and run the experiment at the same condition described earlier, where only a

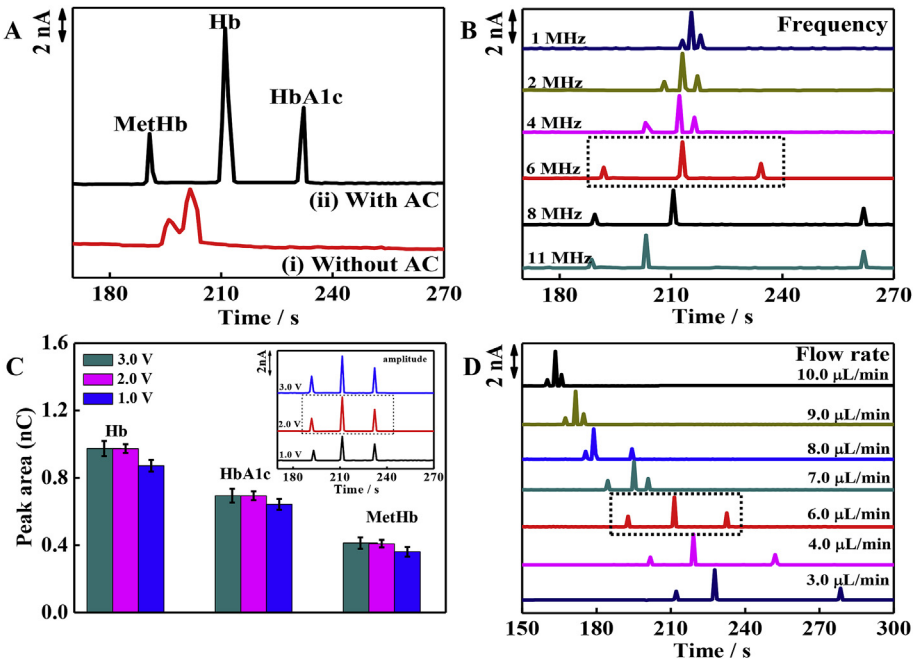

Fig. 3. Electropherograms (A) separation (without (i) and with (ii) AC modulation), (B) the effects of AC frequency, (C) Amplitude (histogram calculated using peak area, inset: signal response of amplitude in different amplitude), and (D) flow rate, separation parameter was 6 μL/min flow rate, 6 MHz frequency and 2V amplitude, and applied potential of −500 mV.

single peak corresponding to Hb was observed at the migration time of 211.4 ± 1.0 s (Fig. S5(i)). Secondly, HbA1c standard solution (Hb, MetHb, and HbA1c) was injected, where a clear peak corresponding to HbA1c appeared at 231.7 ± 1.5 s. In this case, additional small peak observed at 191.1 ± 0.5 s was due to the presence of MetHb in HbA1c standard solution. Based on these results, we assigned MetHb, Hb, and HbA1c migration time as 191.1 ± 0.5, 211.4 ± 1.0, and 231.7 ± 1.5 s, respectively (Fig. S5(ii)). The separation efficiencies for MetHb, Hb, and HbA1c were calculated and expressed in terms of the number of theoretical plates ($N = 5.54(t_R/W_{1/2})^2$) which was found to be 92 352 ± 3125, 50 459 ± 1925, and 136 769 ± 3567 for MetHb, Hb, and HbA1c, respectively. Based on these results the proposed method gives an advantage over the conventional chromatographic and electrophoretic separation of Hb and HbA1c by being simple and faster (< 300 s) in comparison (Mario et al., 1997).

3.4. Calibration plot using standard solution

Under the optimized experimental conditions, the EMSC performance for Hb and HbA1c analysis was demonstrated using chronoamperometry. Fig. 4(A and B) shows the response signals obtained at −500 mV *vs.* Ag/AgCl in deoxygenated 0.1 M PBS containing (A) Hb and (B) Hb, and HbA1c. The results clearly show that the signal increases as their concentrations increase, indicating that the target species have been effectively analyzed by EMSC. As shown in Fig. 4(C), the calibration plot for mere Hb showed two linear ranges from 1.0×10^{-6} to 0.001 mM and from 0.001 to 3.5 mM with the detection limit of $8.1 \times 10^{-7} \pm 3.0 \times 10^{-8}$ mM. The linear regression equations for only Hb was expressed as peak area (nC) = 0.67 (± 0.070) + 5484.49 (± 140.17) (mM) and peak area (nC) = 9.38 (± 0.41) + 36.63 (± 0.80) (mM), with correlation coefficients of 0.998 and 0.997, respectively. Otherwise, for mixed standard solution (containing Hb, HbA1c, and MetHb) (Fig. 4(D)), the dynamic ranges were from 2.0×10^{-6} to 0.001 mM and 0.001–3.0 mM for Hb, and from 3.0×10^{-6} to 0.001 mM and 0.001–0.6 mM for HbA1c, with a detection limit of $8.3 \times 10^{-7} \pm 3.0 \times 10^{-8}$ mM and $9.2 \times 10^{-7} \pm 5.0 \times 10^{-8}$ mM, respectively. The linear dependency of the HbA1c calibration plot yielded two regression equations in a mixed solution, which is expressed as peak area (nC) = 0.13 (± 0.021) + 2409.68 (± 41.21) [HbA1c] (mM) and peak area (nC) = 2.34 (± 0.70) + 52.63 (± 1.00) [HbA1c] (mM), with correlation coefficients of 0.999 and 0.986, respectively. The detection limits were determined to be significantly lower compared to the recently reported (Jain et al., 2017; Hu et al., 2014; Moon et al., 2017). To the best of knowledge, this work is the first report for the simultaneous detection of Hb and HbA1c using an electrochemical microfluidic channel.

3.5. Selectivity and stability of the proposed sensor

The selectivity of EMSC analysis was demonstrated using the species present in a real sample matrix, such as glucose, albumin (~3.5–5.5 g/dL), IgG (~0.8–1.8 g/dL), uric acid, ascorbic acid, dopamine, and fibrinogens (~160–410 mg/dL). The interfering species were examined at the concentration of 0.1, 1.0, and 10.0 μM, where no signal was observed in the present experiments (*i.e.* the migration time), indicating that the EMSC is highly selective for the detection of Hb and HbA1c (Fig. 5(A)). Furthermore, most of the proteins and other biomolecules are separated from Hb in the whole blood during the separation process. EMSC was evaluated by the analysis of Hb and HbA1c in the presence of interfering species together in a mixed sample solution. The sensitivity of Hb and HbA1c detection in this case was 93 ± 4% and 95 ± 3% ($n = 5$), respectively compared when they were detected alone. The reproducibility of the EMSC showed the RSD < 4.6% ($n = 5$) and the electrode-to-electrode RSD was < 3.9%, where the deviation might be resulted from the small variation in the sensor probe fabrication steps and the performance of EMSC. To evaluate the stability of the sensor (Fig. S6), CVs were recorded separately for Hb and HbA1c at regular intervals (7 days) for two months, where 95 ± 3% sensitivity was retained up to eight weeks. Considerable long stability in our case was due to the chemical binding of NB onto a stable conductive polymer layer.

3.6. Determination of Hb and glycated Hb fractions in real blood sample

We performed the real sample experiments using two methods ((i) spiking and recovery test and (ii) standard addition method) to validate the result. In case of spike and recovery method, known concentrations of Hb and HbAlc were spiked in blood and recovered using the EMSC. According to the Table S1, the designed EMSC can detect Hb and HbAlc

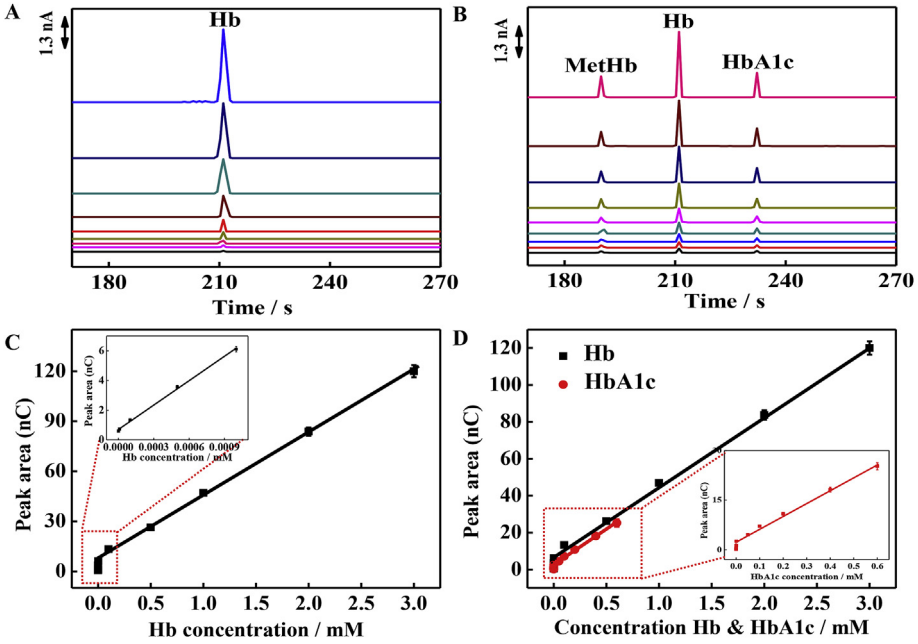

Fig. 4. Electropherograms obtained for varying concentrations of (A) Hb and (B) HbA1c (while Hb 100 nM and 105 nM). Calibration curves (C) Hb and (D) mixed solution Hb and HbA1c obtained by plotting signal in (A) and (B) (D-inset: callibration curves for HbA1c).

effectively in the blood samples at various concentrations. Fig. 5(B) shows the chronoamperogram obtained from human blood sample and standard solution of Hb and HbA1c. Most of the major proteins, except Hb, are electrochemically inactive and do not show the redox reaction with NB. Six additional peaks were observed (black solid line), which were assumed to be from other Hb fractions ($HbAld_{1+2}$, HbAle, HbAld3a, $HbAl_{a+b}$, HbA2, and HbAld3b) that present in the human blood samples, which can be confirmed by expected molecular weight from previously reported paper (Schnek and Schroeder, 1961; Zurbriggen et al., 2005).

To confirm the validation of the method for detection of Hb and HbAlc in the blood samples, the standard addition method was performed. The calibration plot in standard addition method for Hb and HbAlc determination was shown in Fig. 5(C and D). The concentration of Hb was determined to be 2454.2 μM, which is the physiological range of the normal human being (Mann et al., 2010). Similarly, we also calculated the HbAlc concentration in human blood sample which was found to be 93.5 μM. The % HbA1c (as prescribed by "National Glycohemoglobin Standardization Program") value was calculated to be 5.62%, which meets well with the value of normal healthy adults (4–6%) (Liu et al., 2006).

4. Conclusions

We have successfully developed a sensor coupled with AC field applied-microfluidic device for the simultaneous detection of Hb and 8

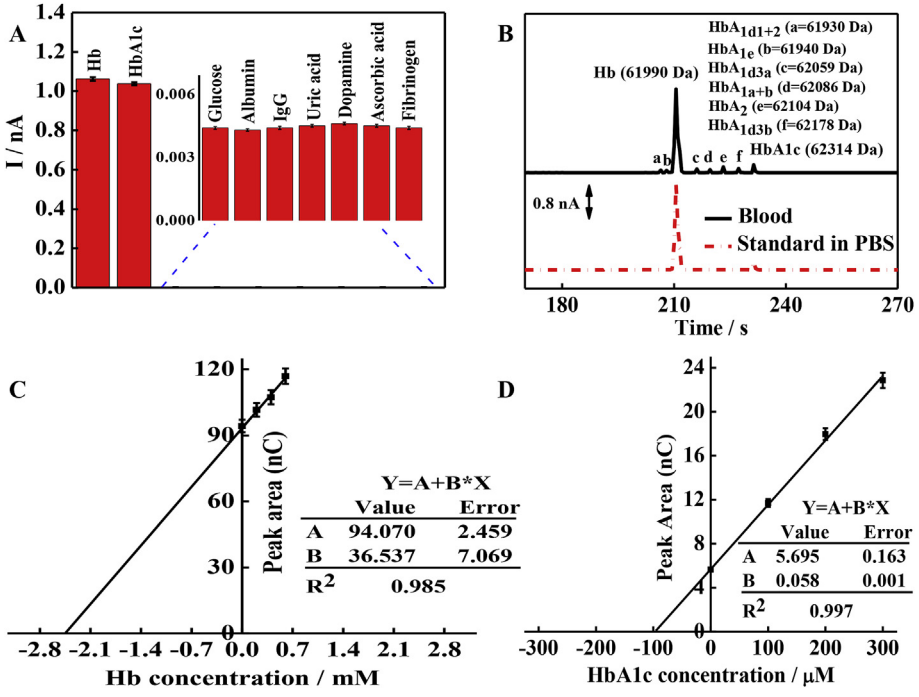

Fig. 5. (A) Histogram showing the selectivity of EMSC, inset shows the magnified view of the interfering molecules. (B) Electrochromatograms obtained for Hb and HbA1c separation in blood sample (black line) and in PBS (red line) ((a–f)) shows the unknown sample peak). Calibration plot using standard addition method obtained for the determination of (C) Hb and (D) HbA1c content in the sample. (For interpretation of the references to colour in this figure legend, the reader is referred to the Web version of this article.)

kinds of glycated Hb fractions in human blood samples. The performance of different catalytic redox mediators (NB, TBO, and NR) were compared and NB was recognized to show the best analytical signal for the detection of Hb and HbA1c. The sensor probe was designed by immobilizing NB onto the conductive polymer-NSPC nanocomposite layer. The proposed device detected Hb and HbA1c simultaneously in a single experimental setup within 140 s. The detection limits of Hb and HbA1c were found to be $8.1 \times 10^{-7} \pm 3.0 \times 10^{-8}$ and $9.2 \times 10^{-7} \pm 5 \times 10^{-8}$ mM, respectively. The separation and detection of Hb and HbA1c were not disturbed by the complex sample matrix. The developed method offers highly precise, selective, ultrasensitive, and fast detections of Hb and glycated Hb fractions in a miniaturized setting without any biological receptors (antibody, aptamer, enzyme, *etc*), thereby offering high throughput detection of Hb and HbA1c in point-of-care analysis.

Declaration of competing interest

The authors declare that they have no known competing financial interests or personal relationships that could have appeared to influence the work reported in this paper.

Acknowledgments

This work was supported by the National Research Foundation of Korea (NRF) grant funded by the Korea government (MSIP) (No. 2019R1A2C1002531). This work was also supported by a grant from the Korea Health Technology R&D Project through KHIDI funded by the Ministry for Health and Welfare of Korea (HI14C1135 & HI15C0987).

Appendix A. Supplementary data

Supplementary data to this article can be found online at https://doi.org/10.1016/j.bios.2019.111515.

References

Abraham, E.C., 1981. Biochim. Biophys. Acta 667, 168–176.
Ang, S.H., Rambeli, M., Thevarajah, T.M., Alias, Y.B., Khor, S.M., 2016. Biosens. Bioelectron. 78, 187–193.
Barman, I., Dingari, N.C., Kang, J.W., Horowitz, G.L., Dasari, R.R., Feld, M.S., 2012. Anal. Chem. 84, 2474–2482.
Borchardt, L., Zhu, Q.-L., Casco, M.E., Berger, R., Zhunag, X., Kaskel, S., Feng, X., Xu, Q., 2017. Mater. Today 20, 592–610.
Dincer, C., Bruch, R., Kling, A., Dittrich, P.S., Urban, G.A., 2017. Trends Biotechnol. 35, 728–742.
Demirci, U., Khademhosseini, A., Langer, R., Blander, J., 2017. Microfluidic Technologies for Human Health. World Scientific Press, Singapore.
Dong, J., Li, S., Wang, H., Meng, Q., Fan, L., Xie, H., Cao, C., Zhang, W., 2013. Anal. Chem. 85, 5884–5891.
Hussain, K.K., Akhtar, M.H., Kim, M.H., Jung, D.K., Shim, Y.-B., 2018. Biosens. Bioelectron. 109, 263–271.
Hussain, K.K., Moon, J.-M., Park, D.S., Shim, Y.-B., 2017. Electroanalysis 29, 2190–2199.
Hu, W.L., Jang, L.S., Hsieh, K.M., Fan, C.W., Chen, M.K., Wang, M.H., 2014. Sens. Actuators B Chem. 203, 736–744.
Jing, Z., Wei-jie, Y., Nan, Z., Yi, Z., Ling, W., 2012. PLoS One 7, e43655.
Jain, U., Gupta, S., Chauhan, N., 2017. Int. J. Biol. Macromol. 101, 896–903.
Kumar, C.S.S.R., 2010. Microfluidic Devices in Nanotechnology: Applications. John Wiley and Sons, Wiley, Hoboken, NJ, US.
Kuo, I.C., Lin, H.Y.H., Niu, S.W., Hwang, D.Y., Lee, J.J., Tsai, J.C., Hung, C.C., Hwang, S.J., Chen, H.C., 2016. Sci. Rep. 6.
Kiran, M.S., Itoh, T., Yoshida, K., Kawashima, N., Biju, V., Ishikawa, M., 2010. Anal. Chem. 82, 1342–1348.
Lafferty, J.D., McFarlane, A.G., Chui, D.H., 2002. Arch. Pathol. Lab Med. 126, 1494–1500.
Lee, K.-S., Shiddiky, M.J., Park, S.H., Park, D.-S., Shim, Y.-B., 2008. Electrophoresis 29, 1910–1917.
Liu, S.Q., Wollenberger, U., Katterle, M., Scheller, F.W., 2006. Sens. Actuators B Chem. 113, 623–629.
Moon, J.-M., Kim, D.-M., Kim, M.H., Han, J.Y., Jung, D.K., Shim, Y.-B., 2017. Biosens. Bioelectron. 91, 128–135.
Mann, D.M., Carson, A.P., Shimbo, D., Fonseca, V., Fox, C.S., Muntner, P., 2010. Diabetes Care 33, 2190–2195.
Mario, N., Baudin, B., Aussel, C., Giboudeau, J., 1997. Clin. Chem. 43, 2137–2142.
Noh, H.B., Chandra, P., Kim, Y.J., Shim, Y.-B., 2012. Anal. Chem. 84, 9738–9744.
Naveen, M.H., Shim, K., Hossain, M.S.A., Kim, J.H., Shim, Y.-B., 2017. Adv. Energy Mater. 7, 1602002.
Rhea, J.M., Molinaro, R., 2014. Am. J. Clin. Pathol. 141, 5–16.
Sackmann, E.K., Fulton, A.L., Beebe, D.J., 2014. Nature 507, 181–189.
Schnek, A.G., Schroeder, W.A., 1961. J. Am. Chem. Soc. 83, 1472–1478.
Tseng, W.L., Hsieh, M.M., Wang, S.J., Chang, H.T., 2000. J. Chromatogr. A 894, 219–230.
Weissbluth, M., 1974. Hemoglobin. In: Hemoglobin. Springer, Berlin, Heidelberg, pp. 10–26.
Zhu, C., Li, H., Fu, S., Du, D., Lin, Y., 2016. Chem. Soc. Rev. 45, 517–531.
Zurbriggen, K., Schmugge, M., Schmid, M., Durka, S., Kleinert, P., Kuster, T., Heizmann, C.W., Troxler, H., 2005. Clin. Chem. 51, 989–996.